

Article

Controlling Nucleation Density While Simultaneously Promoting Edge-Growth Using Oxygen-Assisted Fast Synthesis of Isolated Large-Domain Graphene

Phi H.Q. Pham, Weiwei Zhou, Nhi V Quach, Jinfeng Li, Jian-Guo Zheng, and Peter J. Burke

Chem. Mater., **Just Accepted Manuscript** • DOI: 10.1021/acs.chemmater.6b01826 • Publication Date (Web): 06 Sep 2016Downloaded from <http://pubs.acs.org> on September 8, 2016

Just Accepted

“Just Accepted” manuscripts have been peer-reviewed and accepted for publication. They are posted online prior to technical editing, formatting for publication and author proofing. The American Chemical Society provides “Just Accepted” as a free service to the research community to expedite the dissemination of scientific material as soon as possible after acceptance. “Just Accepted” manuscripts appear in full in PDF format accompanied by an HTML abstract. “Just Accepted” manuscripts have been fully peer reviewed, but should not be considered the official version of record. They are accessible to all readers and citable by the Digital Object Identifier (DOI®). “Just Accepted” is an optional service offered to authors. Therefore, the “Just Accepted” Web site may not include all articles that will be published in the journal. After a manuscript is technically edited and formatted, it will be removed from the “Just Accepted” Web site and published as an ASAP article. Note that technical editing may introduce minor changes to the manuscript text and/or graphics which could affect content, and all legal disclaimers and ethical guidelines that apply to the journal pertain. ACS cannot be held responsible for errors or consequences arising from the use of information contained in these “Just Accepted” manuscripts.

1
2
3
4
5
6
7 Controlling Nucleation Density While
8
9
10
11 Simultaneously Promoting Edge-Growth Using
12
13
14
15 Oxygen-Assisted Fast Synthesis of Isolated Large-
16
17
18
19
20 Domain Graphene
21
22
23
24

25 *Phi H.Q. Pham †, Weiwei Zhou †, Nhi V. Quach †, Jinfeng Li †, Jian-Guo Zheng‡, Peter J.*
26 *Burke* †*
27
28

29
30
31 †Department of Electrical Engineering and Computer Science, University of California, Irvine,
32
33 CA 92697, USA
34
35

36
37 ‡Irvine Materials Research Institute University of California Irvine, CA 92697, USA
38
39
40
41
42
43
44
45
46
47
48
49
50
51
52
53
54
55
56
57
58
59
60

1
2
3 ABSTRACT
4
5
6

7 We report a two-step chemical vapor deposition (CVD) growth method for rapid synthesis of
8 isolated large-domain graphene. The key feature of the two-step growth method is to separate
9 nucleation from growth, performing the nucleation in step-one with a low carbon feedstock
10 (methane) gas flow rate, and rapid growth in step-two with a high flow rate. We find empirically
11 that, even under the high flow rate conditions of step-two, the nucleation density on the inside of
12 the copper pocket used for growth is suppressed (preventing merging of domains into full films)
13 until the graphene growing on the outside of the pocket merges into a full film, fully covering the
14 outside. The mechanism for this suppression is believed to be related to oxygen-assisted
15 passivation of nucleation sites, a decreased energetic barrier for edge-attachment growth, and
16 diffusion of carbon through the copper bulk. These conditions enable us to finely tune the local
17 carbon concentration on the inside surface for fast growth and minimum nucleation density, and
18 achieve a growth of 5-mm isolated graphene domains in under 5 hours of total growth time,
19 much faster than traditional one-step growth methods.
20
21
22
23
24
25
26
27
28
29
30
31
32
33
34
35
36
37
38
39
40
41
42
43
44
45
46
47
48
49
50
51
52
53
54
55
56
57
58
59
60

1
2
3 INTRODUCTION
4

5
6 What is the most rapid, efficient chemical vapor deposition (CVD) method to produce large-
7
8 area, single-domain graphene? This task remains a challenge because rapid growth conditions
9
10 usually result in concomitant high nucleation density, causing merging of domains and
11
12 ultimately, full film coverage¹⁻³, prior to the growth of large domains. This results in multiple,
13
14 detrimental grain boundaries⁴ due to the polycrystalline nature of multi-domain films⁵. The
15
16 ultimate goal, and only way to ensure that no grain boundaries exist within the graphene is the
17
18 synthesis of wafer-scale, isolated single-domains. En route to reaching this goal, researchers
19
20 have developed numerous methods (such as electropolishing copper foils⁶, high pressure
21
22 hydrogen annealing⁷, low methane flow², and oxidized copper growth^{8,9}) to minimize the
23
24 nucleation density. Of these, CVD growth on oxidized copper substrates has proven to be one of
25
26 the most effective^{8,9} at allowing the necessary surface-area and spacing required to avoid
27
28 merging of neighboring domains. However, this method, which relies on low flow rates of the
29
30 carbon feedstock gas, comes at the cost of very long growth times⁸⁻¹², measured in days instead
31
32 of hours.
33
34
35
36
37

38
39 Here, we report a two-step CVD growth method for rapid synthesis of isolated large-domain
40
41 graphene. The key feature of the two-step growth method is to separate nucleation from growth,
42
43 performing the nucleation in step-one with a low feedstock gas (methane) flow rate, and rapid
44
45 growth in step-two with a high flow rate. We find empirically that, even under the high flow rate
46
47 conditions of step-two, the nucleation density is suppressed by the geometry of the copper
48
49 pocket⁶ used, until the outside of the copper pocket is fully covered by a graphene film. During
50
51 step-two (the high growth rate step), we are able to tune the carbon concentration on the inside of
52
53 the copper pocket to be *above* the threshold concentration required for edge growth, but *below*
54
55
56
57
58
59
60

1
2
3 the threshold concentration required for nucleation¹³, even in the presence of high methane flow
4 rates. Operating in this regime produces large-domain graphene without the formation of full
5 films, ensuring that no detrimental grain boundaries develop.
6
7
8
9

10 A unique combination of mechanisms enables us to grow in this regime. While a quantitative
11 model is still not available, the mechanisms involved are believed to include 1) passivation of
12 active nucleation sites through oxidation of the copper surface⁹, 2) reduction of the energy
13 barrier for edge-attachment growth resulting from the de-hydrogenation of methane by the
14 oxidized copper surface⁸, and 3) a unique carbon concentration profile (resulting from the role of
15 carbon sources and sinks at the inside and outside due to nucleation, growth, and diffusion of
16 carbon through the copper bulk¹⁴, in both directions). This “window” has not been explored
17 previously in the literature. Furthermore, we show that this “window” of opportunity exists only
18 when the outside is not fully covered with graphene. Once the outside surface is covered, the
19 nucleation density on the inner surface increases dramatically, and quickly results in fully
20 merged films with grain boundaries, rather than isolated single domains (the goal of this work).
21 Using this approach, we demonstrate growth of 5-mm isolated graphene domains in less than 5
22 hours of total growth time, much faster than traditional one-step growth methods.
23
24
25
26
27
28
29
30
31
32
33
34
35
36
37
38
39
40

41 RESULTS

42
43 We performed CVD graphene growth using enclosed copper pockets due to the improved
44 surface conditions and decreased diffusivity, and hence, decreased nucleation and growth rate in
45 the interior surface as reported in previous CVD studies^{2,6,14}. Our findings regarding diffusion
46 from the inside surface to the outside surface of the copper pocket will be discussed in depth,
47 later in the paper. Briefly, a copper pocket is used, and large-domains grow on the inside. Our
48 studies show a critical role of the surface coverage of the outside surface influencing growth on
49
50
51
52
53
54
55
56
57
58
59
60

1
2
3 the inside, elucidated in detail below. Preparation of the enclosed copper pocket is documented
4
5 in the methods and supporting information (**Fig. S1**). Before growth optimization (two-step
6
7 growth) experiments were conducted, we monitored and adjusted pre-growth conditions
8
9 (excluding methane flow rate) to achieve the lowest nucleation density possible. These results
10
11 including oxidation conditions^{8,10}, annealing conditions^{7,9}, and heating gases^{11,12} are documented
12
13 in (**Fig. S2**). These parameters are held constant throughout the remainder of experiments
14
15 including two-step growth studies (**Fig. S3**).
16
17
18

19
20 Typically, for one-step growth procedures, a low methane flow rate is used over long durations
21
22 in order to keep the nucleation density low⁸⁻¹². This methodology to achieve low nucleation
23
24 density comes at the cost that the growth rate is also low⁸⁻¹², especially since the growth rate
25
26 decreases overtime¹⁵. As verified in (**Fig. S4a-b**), when using a low methane flow rate (.4 sccm),
27
28 distinct mm-sized domains appear in low density (**Fig. S5a-b**), but long growth durations have
29
30 limited effects on increasing domain size. To assess if a high methane flow rate could be used to
31
32 synthesis large-domain graphene, we performed a series of one-step growths using elevated
33
34 methane flow rates (1.6 sccm) to probe the domain-size and nucleation density overtime (**Fig.**
35
36
37
38 **1a**). Following growth, the enclosed copper pockets are cut open, and oxidized on a hotplate to
39
40 reveal graphene growth coverage¹⁶. (**Fig. 1b-d**) shows a depiction and experimental verification
41
42 that using elevated methane flow rates can noticeably increase the graphene domain-size, but due
43
44 to the increased nucleation density (**Fig. S5c-d**), results in the formation of merged domains, and
45
46 ultimately, continuous graphene films, as the growth duration proceeds. From these control
47
48 studies, we confirm that in order to synthesize large-domain graphene using an increased
49
50 methane flow rate (in order to decrease the overall growth duration), without the detriment of
51
52
53
54
55
56
57
58
59
60

increased nucleation density (which would limit the ultimate size of isolated graphene domains), a traditional one-step growth protocol is not adequate.

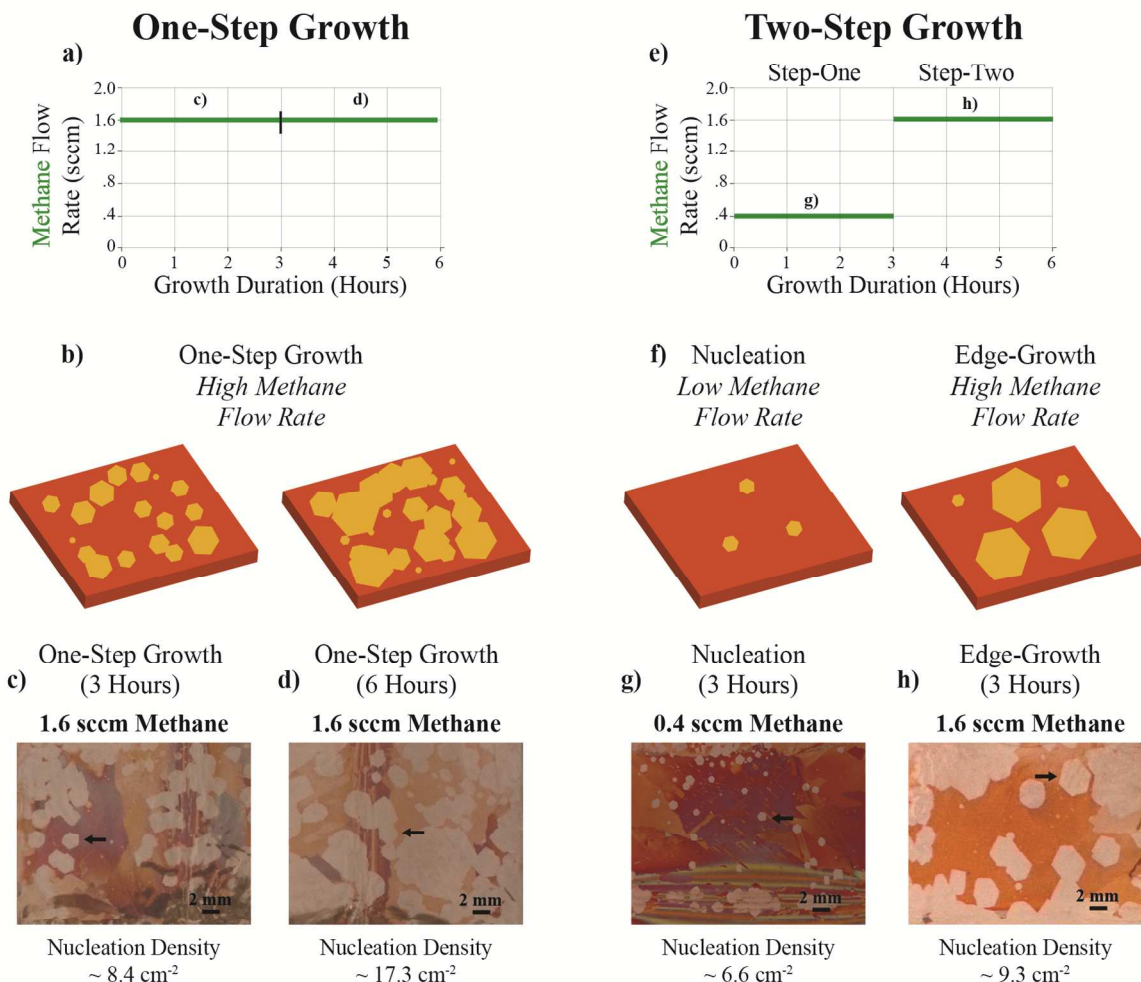


Figure 1. a) Outline of typical one-step growth, using high methane flow rate b) cartoon depicting graphene growth using high methane flow rate resulting in high nucleation density, which forms full films after long duration. c-d) Optical images of oxidized copper after one-step growth for 3-hour, and 6-hour duration. e) Outline of two-step growth, using low methane flow rate stage, followed by high methane flow rate stage. f) Cartoon depicting graphene growth using two-step growth. Step-one creates a low nucleation density by using low methane flow rates. Step-two promotes edge-growth using elevated methane flow rates. g-h) Optical images of

1
2
3 oxidized copper after step-one, and step-two. Step-one (.4 sccm) produces domains of low
4 nucleation density; step-two (1.6 sccm) increases the size of isolated domains. Black arrows
5
6 point to graphene domains.
7
8
9

10
11 The two-step growth protocol employed here, outlined in **(Fig. 1e)**, consists of a low methane
12 flow rate stage, followed by a high methane flow rate stage. Argon and hydrogen flow rates are
13 kept constant throughout the entire growth duration. Step-one is intended to achieving a low
14 nucleation density in order to allow the adequate surface area to grow isolated, large-area single-
15 domain graphene, whereas step-two is aimed at enlarging the size of existing nucleated domains
16 **(Fig. 1f)**. Previous studies using two-step growth were designed to increase the nucleation
17 density after large-domain graphene was synthesized in order to fill-in voids, and ultimately,
18 create large-domain films³, whereas our main aim is to avoid merging of domains by maintaining
19 a low nucleation density. **(Fig. 1g-h)** shows growths after step-one, and step-two, and
20 demonstrates that despite the increased growth rate (from the increased methane flow rate)
21 during step-two, the nucleation density is does not dramatically increase **(Fig. S5g)**, such that
22 isolated domains are still apparent. The mechanisms that enable these experimental results are
23 believed to be related to the diffusion of carbon species in copper, specifically to copper pocket
24 growths, and will be discussed in detail below. Regardless of the mechanism, by using our two-
25 step growth process, we are able to synthesize isolated, 5-mm single-domain graphene in less
26 than 5 hours.
27
28
29
30
31
32
33
34
35
36
37
38
39
40
41
42
43
44
45
46
47

48
49 Following two-step synthesis, we employed a series of characterization techniques to assess
50 the quality of the synthesized graphene, and to fully confirm that the graphene is neither
51 polycrystalline nor multilayer. First, scanning electron microscopy (SEM) was used to image
52 graphene on the copper foils; we found that the 120-degree angle of the domain growth front,
53
54
55
56
57
58
59
60

1
2
3 and the lack of observable defects or boundaries highly advocate that the synthesized graphene is
4 single-domain⁷ as shown in **(Fig. 2a)**. Optical images of transferred^{17,18} single-domains onto
5 silicon oxide (SiO₂) show that the majority of the domain area is monolayer, with only a small
6 nucleation center consisting of ad-layer graphene present **(Fig. 2b)**. To further substantiate the
7 growth of monolayer, single-domain graphene, we used selected area electron diffraction
8 (SAED) to investigate the crystal structure of domains transferred^{17,18} onto Transmission
9 Electron Microscopy (TEM) grids. **(Fig. 2c)** shows a typical SAED pattern, recorded from one
10 single domain and verifies that the graphene domain is single crystal¹⁹. **(Fig. S6)** shows a
11 collection of SAED patterns from one single-domain spanning 2 mm². The alignment angle of
12 the electron diffraction patterns are within 2 degrees of variation (the single domain graphene
13 was laid on a copper TEM grid, and as a consequence, patterns recorded across large distances
14 vary from bending of the TEM grid) and further supports the growth of single-domains^{5,7}.
15 Raman spectroscopy was used to assess the quality of single-domain graphene transferred onto
16 an OctadecylTriChloroSilane (ODTS) modified SiO₂ substrate (as to minimize substrate
17 effects)²⁰. **(Fig. 2d)** shows a representative Raman spectra of a single-domain. **(Fig. 2e-g)** shows
18 the intensity of the G-peak (~1583), 2D-peak(~2683), and the D-peak (~1350) collected for a
19 sample using Raman mapping, respectively²¹. In all 3 intensity-mapping images, a clear
20 boundary between the graphene and the substrate is obvious. A small patch of PMMA
21 contamination near the bottom of the graphene sample is also evident²². The lack of D-peak²³
22 (except around the graphene boundary, and PMMA contamination), in addition to the large ratio
23 of 2D:G intensities^{22,24} (> 3:1) **(Fig. 2h)**, indicates a very high quality monolayer of graphene.
24 Altogether, our characterization methods confirm that the synthesized graphene using two-step
25 growth is monolayer, and single-domain.
26
27
28
29
30
31
32
33
34
35
36
37
38
39
40
41
42
43
44
45
46
47
48
49
50
51
52
53
54
55
56
57
58
59
60

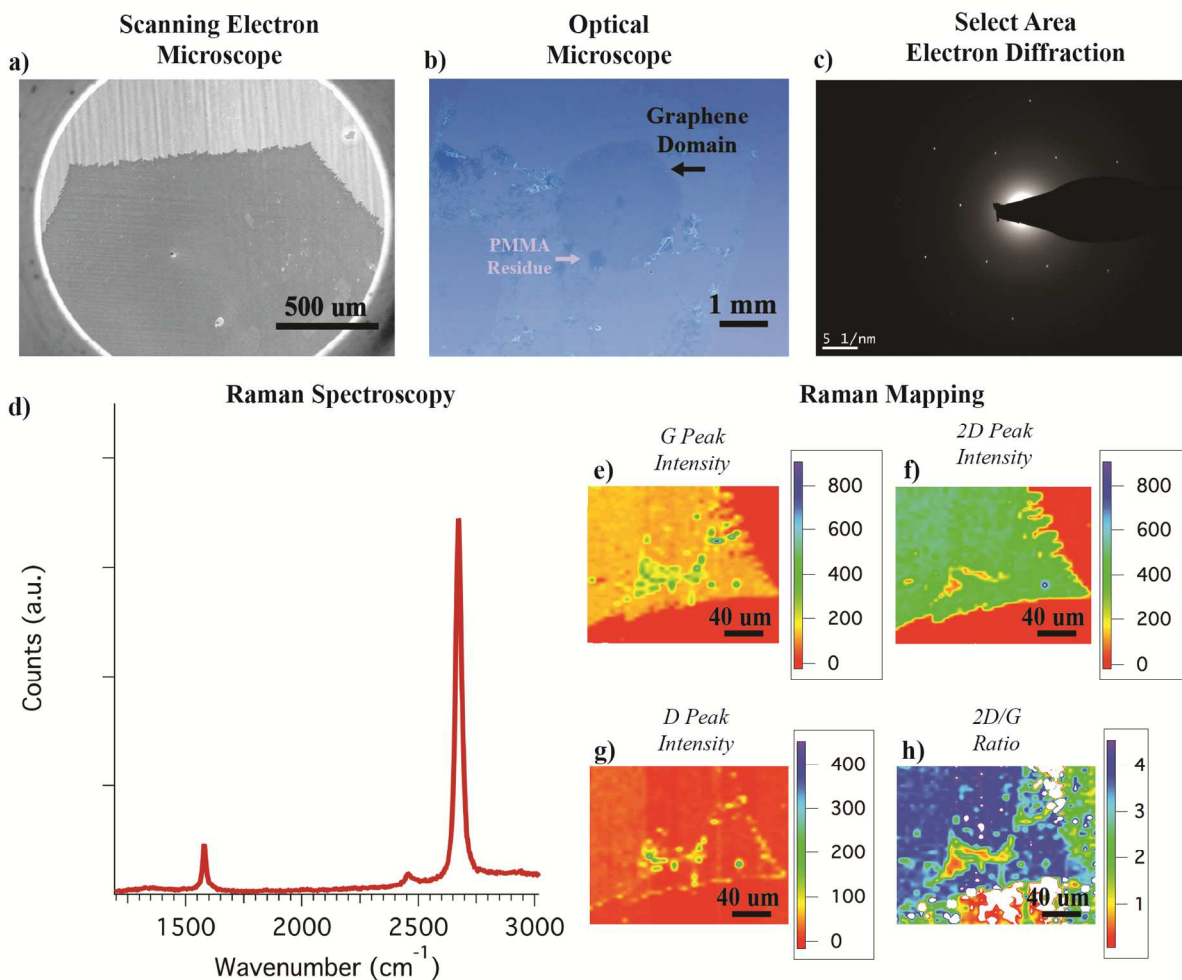


Figure 2: a) SEM image of hexagonal growth edge of large-domain graphene synthesized using two-step growth. b) Optical image of large-domain graphene transferred onto SiO₂ substrate. The majority of the domain is monolayer, with a small observable nucleation center consisting of adlayer graphene. c) A representative SAED pattern of one single-domain showing the single crystal nature of the domain. d) A representative Raman Spectra of monolayer graphene e-g) Raman mapping images of single-domain graphene on a domain corner to spatially track intensities of the G peak, 2D Peak and D Peak, respectively. Defects are observed on a small patch of PMMA contamination near the bottom edge of the domain, and on the domain-edge. h)

The ratio of the intensity of the 2D:G peaks is greater than 3:1 for the majority of the single-domain, and further confirms high quality, monolayer graphene is synthesized.

To investigate the dependence on the methane flow rate during two-step growth, we performed a series of growths, varying the methane flow rate using the two-step process. Step-one, and step-two were both held for 3-hour duration each. (Fig. 3a) shows an optical image of the inside surface of the copper pockets after 3 hours of low methane exposure (step-one growth). Distinct mm-sized domains appear spread across the inside surface, with the adequate spacing necessary for edge-growth during step-two (Fig S5a).

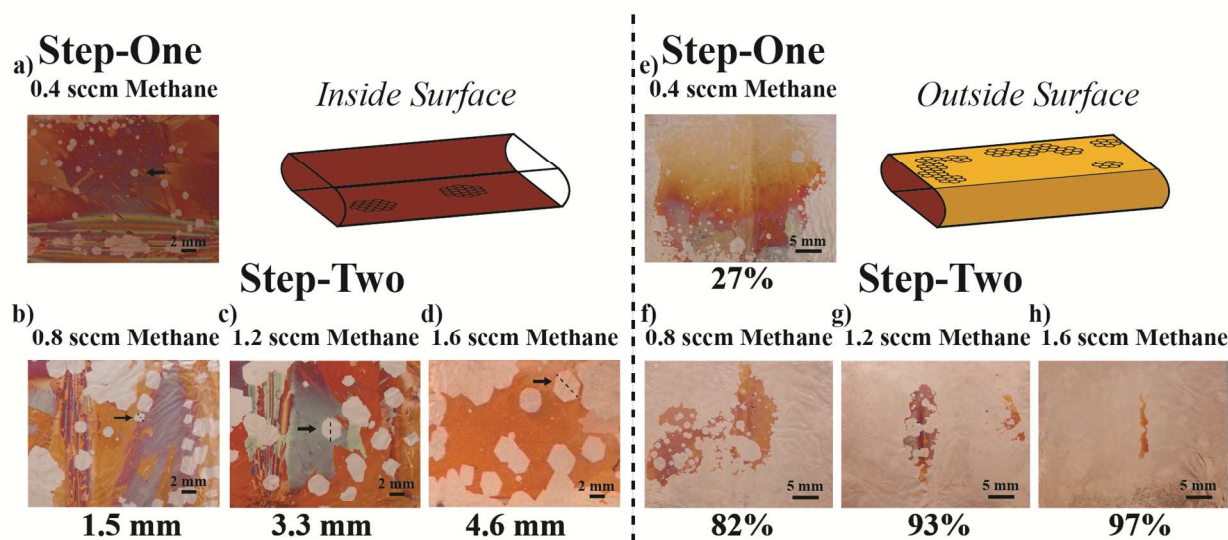


Figure 3: a) Optical image of graphene on the inside of copper pockets following copper oxidation after step-one. Step-one uses low methane flow (.4 sccm) over 3 hours to create low density of nucleation. b-d) Optical images of graphene on the inside of copper pockets following copper oxidation after two-step growth varying the second-step flow rate from .8, 1.2, to 1.6 sccm, respectively. By increasing the methane flow rate (for step-two) the average domain-size increases, without the need to increase growth duration. e-h) Optical images of graphene on the outside of copper pockets following copper oxidation after step-one and step-two. Increases in

1
2
3 methane flow rate (step-two) causes an increase of growth on the outside, with greater percent
4 coverage for greater methane flow rate. Using 1.6 sccm methane for the step-two flow rate (for 3
5 hours) results in nearly full coverage of the outside surface. Black arrows point to graphene
6 domains.
7
8
9
10
11

12
13 After defining the low nucleation density set in step-one, we monitored the effects of
14 increasing the flow rate for step-two. **(Fig. 3b-d)** shows a series of optical images of the inside of
15 the copper pockets after two-step growth using identical conditions for the step-one (.4 sccm),
16 but with increasing methane flow rate for the second step, ranging from .8 – 1.6 sccm,
17 respectively. Interestingly, by using a two-step growth process, we do not observe a dramatic
18 increase in the nucleation density of graphene domains to the extent that isolated domains exist,
19 even though the methane flow rate is increased incrementally for each experiment **(Fig. S5e-g)**.
20 Moreover, as the second-step flow rate is increased, from .8 to 1.2, and then to 1.6 sccm, the
21 average domain-size increases for respective increases in flow rate, without the need to increase
22 the growth duration.
23
24
25
26
27
28
29
30
31
32
33
34
35
36

37 Using a two-step growth, it is possible to control the size of large-area single-domains by
38 choosing the corresponding step-two methane flow rate. Compared to the single-step growth
39 using low methane flow (.4 sccm) **(Fig. S4b)**, using a two-step growth over the equivalent
40 growth duration, results in larger domain-sizes (for all flow rates, .8, 1.2, and 1.6 sccm).
41 Furthermore, the increase in methane flow rate effectively increases the graphene domain-size,
42 without the expense of additional ad-layer coverage **(Fig. S7)**. Thus, we have shown that by
43 using a two-step growth protocol, it is feasible to promote domain-edge growth while
44 simultaneously controlling the nucleation density.
45
46
47
48
49
50
51
52
53
54

55 DISCUSSION

56
57
58
59
60

1
2
3 Why does the nucleation density not increase with an increase in the step-two methane flow
4 rate as revealed in our experiments? The use of high methane flow rate to grow large-domain
5 graphene while retaining a low nucleation density seems contradictory to previous
6 experiments^{2,3,7-12,16}, and indicates that other factors play a key role in limiting the overall
7 nucleation density inside the copper pocket. To investigate why elevated methane flow rates
8 could result in low nucleation density instead of full graphene films, we monitored graphene
9 growth both on the inside and outside surface of the copper pocket following two-step growth.
10 We observe that after step-one (**Fig. 3e**), the majority of the outside surface remains uncovered
11 (27% surface coverage); as the flow rate is increased from 0.8 sccm, up to 1.6 sccm for step-two,
12 we notice that the surface coverage of the copper foil subsequently increases, up to nearly full
13 coverage (97%) for the largest flow rate (**Fig. 3f-h**). Clearly, increases in step-two methane flow
14 rate increase the overall growth rate^{2,13,15}, generating the increase in domain-size on the inside
15 surface, and increasing coverage on the outside surface.
16
17
18
19
20
21
22
23
24
25
26
27
28
29
30
31
32
33

34 We found a significant transition occurs whenever the outside surface was fully covered. When
35 we used step-two flow rates larger than 1.6 sccm (97% outside surface coverage), such as 2.4
36 sccm, the inside surface contains merged graphene domains, not isolated single-domains (**Fig.**
37 **4a-b**). This apparent increase in nucleation density corresponds to full graphene coverage on the
38 outside surface (100%). These results provide an important clue on how two-step growth
39 preserves a low nucleation density inside the copper pocket during elevated methane flow rates.
40 To assess if the formation of a full film on the outside surface is related to the increase of the
41 nucleation density inside, or merely a result of using elevated methane flow rates, we
42 investigated the influence of the growth duration of step-two, maintaining elevated methane flow
43 rates.
44
45
46
47
48
49
50
51
52
53
54
55
56
57
58
59
60

1
2
3 The increased growth rate that occurs from using elevated methane flow rates results in faster
4 coverage of the outside surface; thus, by decreasing the overall growth duration we are able to
5 probe the influence of elevated methane flow on the nucleation density on the inside surface,
6 before a full film exists on the outside. Despite using high methane flow rates (2.4 sccm),
7 reducing the growth duration of step-two (from 3 hours to 1.5 hours) to avoid formation of a full
8 film on the outside, results in the growth of isolated, large-domain graphene on the inside surface
9 **(Fig. 4c-d)**. Similar results tuning the growth duration to avoid full film coverage are shown in
10 **(Fig. S8a-d)** for an additional elevated methane flow rate. Thus, we show that the nucleation
11 density inside remains low, only when the outside surface remains uncovered (by adjusting
12 methane flow rate, or growth duration). We have verified this method of synthesizing isolated
13 large domains with over 80 successful growth runs. Regardless of the mechanisms dictating this
14 trend, we can exploit the fast growth rate (using high methane flow rates) and curb the increase
15 of nucleation density by avoiding full film coverage on the outside surface, in parallel. This
16 allows the overall growth duration to be severely reduced when synthesizing isolated large-
17 domain graphene. **(Fig. 4e)** shows an optical image of the inside of a copper foil following a
18 two-step growth with only a 4.5-hour (total) growth duration. We are able to grow isolated,
19 large-domain graphene up to 5 mm in domain-size utilizing the high methane flow rate of step-
20 two, and by tuning the growth duration to avoid full films on the outside to keep nucleation low
21 inside. The majority of the growth duration is the slow, step-one stage (3 hours), where low
22 nucleation density is first established. Compared to other methods that utilize only a single-step
23 growth on oxidized copper substrates, our two-step growth method can be up to 10 times faster
24 than conventional, one-step methods⁸⁻¹² **(Fig. 4f)**. Until the ultimate goal of a wafer-scale single-
25 domain graphene without grain boundaries is achieved, for various large-area graphene
26
27
28
29
30
31
32
33
34
35
36
37
38
39
40
41
42
43
44
45
46
47
48
49
50
51
52
53
54
55
56
57
58
59
60

1
2
3 applications where grain boundaries could be detrimental, continuous monolayer films of merged
4 large-domains can be useful. Using our two-step method, it is simple to grow a full film (as
5 shown in Fig. 4a) consisting of large-domain graphene on the inside surface of the copper pocket
6 by extending the growth duration. The growth of continuous large-domain films and
7 characterization of the large-domain grain boundaries (mm-scale) is documented in **(Fig. S9)**.
8 Altogether, by simultaneously controlling nucleation density and edge-growth, the synthesized
9 graphene demonstrated here highlights the versatility, in terms of domain-size, growth duration,
10 and continuous surface coverage, of the developed growth protocol.
11
12
13
14
15
16
17
18
19
20
21
22
23
24
25
26
27
28
29
30
31
32
33
34
35
36
37
38
39
40
41
42
43
44
45
46
47
48
49
50
51
52
53
54
55
56
57
58
59
60

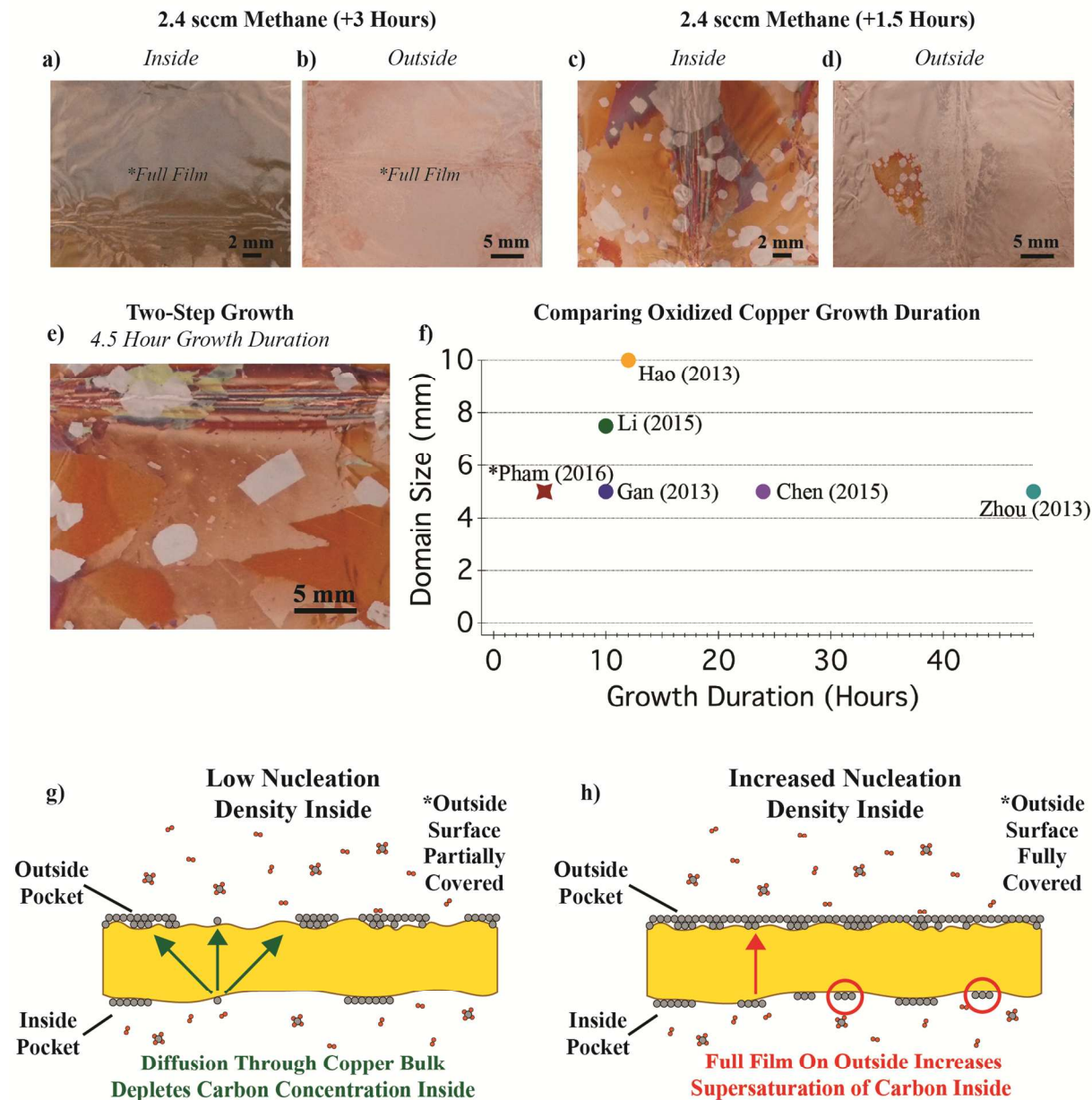


Figure 4: a-b) Optical images of inside and outside of copper pockets following copper oxidation after two-step growth. After full films cover the outside surface, growth inside produces merged domains/films. c-d) Full film coverage on the outside surface is avoided by reducing the growth time to 1.5 hours for step-two using 2.4 sccm. We observe preservation of low nucleation density inside after decreasing growth duration. e) Optical image of inside of copper pockets following copper oxidation after optimized two-step growth resulting in isolated

1
2
3 5-mm graphene domains. f) Comparing other oxidized copper growth durations (one-step)
4 compared to our two-step growth. g-h) Cartoon depicting the influence on the diffusion of
5 carbon and the inside nucleation density, before and after the formation of full films on the
6 outside surface. After formation of a full film on the outside surface, the nucleation density
7 inside, increases.
8
9

10
11
12
13
14
15
16 In order to postulate how the formation of a full film on the outside surface influences the
17 nucleation density on the inside surface, we must consider the conditions whence nucleation
18 occurs. Verified both by observations in our two-step studies, and in the literature, growth inside
19 enclosed copper pockets has the characteristic trend of low nucleation density inside, resulting in
20 larger domains on the inside surface than the outside surface^{2,6,8,10}. Nucleation, in addition to
21 edge-attachment, and ad-layer growth, results from the diffusion of carbon species on the copper
22 surface^{13,14,25-35}. The formation of large carbon chains and clusters responsible for graphene
23 nucleation³²⁻³⁵ occurs when the concentration of carbon species on the surface, C_{Surface} , is much
24 higher compared to the equilibrium concentration ($C_{\text{Nucleation}} \approx 2C_{\text{Equilibrium}}$)^{13,28}. On the other
25 hand, if the level of carbon species is between the nucleation and equilibrium concentrations
26 ($C_{\text{Nucleation}} > C_{\text{Surface}} > C_{\text{Equilibrium}}$), edge-growth of graphene can occur^{13,28,30-34}.
27
28
29
30
31
32
33
34
35
36
37
38
39
40
41

42 Our results suggest that, during step-one where we use a low methane flow rate, the
43 concentration of carbon species on both surfaces remains close to the equilibrium concentration
44 ($C_{\text{Surface}} \geq C_{\text{Equilibrium}}$), thus, in order to cause supersaturated nucleation, long growth durations (3
45 hours) are required. As soon as nucleation occurs, the amount of supersaturated carbon species
46 quickly depletes¹³; hence, the low nucleation density on the inside surface^{13,28}. This assumption
47 is further supported by the nearly bare, outside surface. During step-two, when the methane flow
48 rate is increased, we observe a dramatic increase of domain-size on the inside surface, with
49
50
51
52
53
54
55
56
57
58
59
60

1
2
3 negligible increase in nucleation density. This suggests that the carbon concentration on the
4
5 inside surface still remains in the sensitive region between equilibrium and nucleation, ($C_{\text{Nucleation}}$
6
7 $> C_{\text{Inside}} > C_{\text{Equilibrium}}$)^{13,28}. The increasing coverage on the outside surface (for increasing methane
8
9 flow rate) also agrees with a rise in the carbon concentration. It is observed that new nucleation
10
11 sites on the inside surface do arise, but overall, since we are able to yield isolated domains,
12
13 nucleation does not dominate, and indicates that the carbon concentration level remains close to,
14
15 or below the nucleation threshold. Finally, after a full film is grown on the outside surface,
16
17 indicating that the carbon concentration has remained above the equilibrium level over long
18
19 durations¹³, we observe increased growth on the inside surface, which results in the formation of
20
21 merged domains.
22
23
24
25

26
27 From our experiments adjusting growth duration to compensate for the elevated methane flow
28
29 rates, we observed that full film coverage on the outside surface acts as a convenient, observable
30
31 threshold where nucleation inside remains low, such that isolated domains are synthesized. This
32
33 suggests that, on the inside surface, before the formation of a full film, the concentration of
34
35 carbon species is still relatively close to the nucleation threshold, ($C_{\text{Surface}} \leq C_{\text{Nucleation}}$);
36
37 subsequently, after the formation of a full graphene film on the outside, we observe an increase
38
39 in nucleation density on the inside, suggesting the carbon concentration on the inside increases,
40
41 up to the nucleation threshold^{13,28}. The tuning of growth duration would hence not be effective in
42
43 limiting nucleation on the inside if the concentration of carbon species were well above the
44
45 nucleation threshold before the formation of a full film on the outside, as would be in the case of
46
47 extremely high methane flow rates. This regime is where previous two-step studies have
48
49 typically operated³, and we confirm these results in **(Fig. S8e-h)**. Nonetheless, for our control
50
51 experiments avoiding formation of full film coverage on the outside surface to limit the
52
53
54
55
56
57
58
59
60

1
2
3 nucleation density inside, before formation of a full film on the outside surface, we believe that
4
5 the carbon concentration inside is still within the sensitive range between growth and nucleation.
6
7 Thus, it is plausible that the formation of a full film on the outside, could affect the concentration
8
9 of surface carbon species on the inside to a large enough degree, such that, distinct changes in
10
11 the nucleation rate occur. We speculate that the ability to operate in such a sensitive carbon
12
13 concentration range is only enabled by the unique effects of oxidized copper growth, which are
14
15 utilized during the two-step synthesis.
16
17
18
19

20 Although the growth pathways for CVD graphene synthesis have been widely studied both
21
22 experimentally and theoretically^{3,7,13,25-36}, the exact evolution of graphene growth is still not fully
23
24 developed, especially for oxidized copper growths^{8,9,12,14}. Recently, it has been revealed that the
25
26 presence of surface oxygen species not only limits the nucleation density^{8,9,12}, but also plays a
27
28 crucial role in decreasing the edge-attachment barrier for domain growth⁸, and imperative to our
29
30 studies using copper pockets, enables the diffusion of carbon monomers through the copper
31
32 bulk¹⁴. While the control of the nucleation density via passivation of active nucleation sites has
33
34 been exploited in other studies growing large-domain graphene⁸⁻¹², the use of elevated methane
35
36 flow rates in our studies directly utilizes the decreased edge-attachment barrier for domain
37
38 growth. When using elevated methane flow rates for two-step growth, due to the decreased edge-
39
40 attachment barrier, we expect that the surface carbon species can easily be incorporated into
41
42 existing domains to contribute to edge growth⁸. This is supported by the fact that we see an
43
44 increase in domain-size for increased methane flow rate. We observe this oxygen assisted edge-
45
46 growth, despite the presence of hydrogen gas flow, which can act as a growth inhibitor^{30,31}.
47
48 Furthermore, with an increase in methane flow rate, we observe a variety of isolated, domain
49
50 morphologies, instead of compact hexagons, which further supports utilization of an oxygen
51
52
53
54
55
56
57
58
59
60

1
2
3 aided, decreased edge-attachment barrier and diffusion limited growth⁸, and suggest the observed
4 domain morphologies are not directly dictated by substrate aligned growth^{35,36}. This aspect of our
5 method is dually advantageous, since carbon species that are incorporated into existing domains
6 can quickly deplete the overall concentration of surface carbon species, preventing further
7 nucleation^{8,13,28,31}. In addition, metal step-edges, which often act as sites for nucleation, do not
8 effectively trap carbon monomers³³; therefore, the complete dehydrogenation of CH₄ to carbon
9 monomers from oxygen species⁸ could play a role in decreasing the nucleation density. For these
10 reasons, a two-step growth on oxidized copper is ideal for limiting the nucleation density, since
11 existing domains from step-one can easily incorporate and deplete the surface carbon species
12 during step-two, resulting in a lower nucleation density compared to a one-step growth of
13 equivalent methane flow rate and growth duration (Fig. S5e-f).
14
15
16
17
18
19
20
21
22
23
24
25
26
27
28

29 Due to the fact that our two-step method utilizes oxidized copper growth, which results in the
30 full dehydrogenation of methane to readily yield carbon monomers, diffusion of carbon through
31 the copper bulk is expected to occur^{14,31}; this could be the underlying mechanism controlling
32 increases in the nucleation density on the inside, after a full film covers the outside surface. Even
33 before full film coverage, we observe areas of adlayer graphene growth on the outside surface of
34 the copper pocket for all methane flow rates (**Fig. S10**). Since adlayer growth on the outside
35 surface results from the diffusion of carbon monomers originating from the inside surface^{14,29},
36 our observations suggest that during the two-step process, diffusion through the copper bulk
37 occurs without the need for full film coverage. These results are markedly different compared to
38 previous experiments where the formation of adlayer graphene only takes place after a full film
39 forms on the outside surface^{14,29}. Although the diffusion of carbon through the copper bulk
40 before full film conditions (on the outside surface) has not been established, the evidence
41
42
43
44
45
46
47
48
49
50
51
52
53
54
55
56
57
58
59
60

1
2
3 suggests that the diffusion rates could depend on a number of factors on both surfaces, including
4 the nucleation density, exposed copper surface areas, adlayer nucleation density, and
5 concentration of surface oxides^{14,29-31}, but the optimization of these parameters is beyond the
6 scope of this paper. However, our observations of distinct variations (in domain size and
7 coverage) in adlayer growth on the outside surface (Fig S10) indicate that the diffusion of
8 carbon, feeding adlayer growth on the outside can be altered upon changes in the methane flow
9 rate; thus it is reasonable to speculate that the real time diffusion of carbon species through the
10 copper bulk can influence the local carbon concentration on the inside surface during growth.
11
12
13
14
15
16
17
18
19
20
21

22 One possible explanation of why the nucleation density remains low on the inside surface
23 before full film conditions during two-step growth is that the diffusion of carbon through the
24 copper bulk can “store” excess carbon as adlayer growth where metal defects or impurities
25 exist^{31,33}. Increases in the carbon concentration on the inside surface during two-step growth
26 could thus drive the diffusion rate through the copper bulk¹⁴. This allows the local carbon
27 concentration on the inside to remain below the nucleation threshold as carbon species are
28 depleted from the inside surface (**Fig. 4g**). After the formation of a full film, we observe an
29 increase in the nucleation density on the inside surface (implying an increase of the local carbon
30 concentration) (**Fig 4h**). We have not confirmed where the increase of the carbon concentration
31 arises from, but consider that a decrease of carbon diffusion through the copper bulk could result
32 as a consequence of a decreased concentration gradient as adlayer coverage increases on the
33 outside surface¹⁴. This hypothesis that the diffusion rate through the bulk is determined by full
34 film conditions (such as nucleation density, copper surface coverage) is consistent with previous
35 studies demonstrating a correlation of the inside nucleation density to adlayer coverage on the
36 outside surface²⁹. Further investigation on the diffusion mechanism during two-step growth
37
38
39
40
41
42
43
44
45
46
47
48
49
50
51
52
53
54
55
56
57
58
59
60

1
2
3 could foster development of new methods to severely suppress nucleation on the inside surface,
4
5 and improve bilayer synthesis on the outside surface.
6
7

8 The methods and techniques developed here, simultaneously controlling nucleation density
9
10 and edge growth, should be adapted to other graphene growth substrates to further extend current
11
12 single-domain size limits and rates. The fast two-step growth protocol for growing large single-
13
14 domain graphene can be easily modified to other metallic growth substrates, where graphene
15
16 nucleation and edge growth can be separated into two steps, including but not limited to
17
18 platinum, ruthenium, iridium, and palladium³⁷⁻³⁹. The increased catalytic activity for CH₄ and H₂
19
20 dissociation on platinum for example³⁷, could provide additional means for accelerating the
21
22 growth rates of graphene single-domains when used in combination with a two-step protocol.
23
24 Additionally, the two-step growth method could realize the synthesis of large-domain graphene
25
26 from the seamless stitching of aligned graphene nucleation centers³⁵.
27
28
29
30

31
32 Methods to limit the nucleation density and growth rate by controlling the carbon diffusion
33
34 through the bulk, as investigated in this work, could be further examined using metals such as
35
36 nickel⁴⁰, where the increased carbon solubility, and carbon segregation growth mechanism could
37
38 provide an obvious means to regulating the local carbon concentration, and hence, large-domain
39
40 graphene growth. Methods using nickel and ruthenium substrates under controlled carbon
41
42 segregation conditions have already demonstrated utility for growing mm-scale monolayer
43
44 domains^{41,42}; combined with the techniques developed here on copper, it is reasonable to
45
46 anticipate metals such as these (as alloys, layered stacks, or pure metals) as appropriate growth
47
48 substrates for synthesis of wafer-scale single-domain monolayer graphene or large-domain
49
50 bernal stacked graphene.
51
52
53

54
55 CONCLUSION
56
57
58
59
60

1
2
3 We have demonstrated a simple method for fast synthesis of mm-domain-size graphene using
4 a two-step oxidized copper growth inside copper pockets. The two-step approach, which is
5 supported from oxidative-assisted mechanisms to control nucleation, promote edge growth, and
6 drive carbon diffusion through the copper bulk, exploits the low nucleation density using low
7 methane flow rates, which are then enlarged using increased methane flow rates. We find that the
8 outside surface of the copper pocket acts as an observable threshold where the nucleation density
9 remains low inside. Thus, we can easily tune the first and second stage durations and methane
10 flow rates according to the coverage on the outside copper surface to obtain isolated, large-
11 domain graphene. Applying this method, we show that 5-mm single-domains can be synthesized
12 in 4.5 hours of growth. A host of characterization techniques were employed to confirm that the
13 synthesized graphene is monolayer and single-domain. Our studies focused on optimizing
14 growth conditions can be adapted to most existing CVD systems, and will promote the
15 development of synthesizing wafer-scale single-domain graphene, which will further stimulate
16 advances in graphene integration and applications.
17
18
19
20
21
22
23
24
25
26
27
28
29
30
31
32
33
34
35
36
37
38
39
40
41
42
43
44
45
46
47
48
49
50
51
52
53
54
55
56
57
58
59
60

Supporting Information.

Supporting Information Available: Methods, pre-growth optimization, additional characterization, and nucleation density assessment and controls. This material is available free of charge via the Internet at <http://pubs.acs.org>.

Corresponding Author

Address Correspondence to pburke@uci.edu

Author Contributions

The manuscript was written through contributions of all authors. All authors have given approval to the final version of the manuscript.

Conflict of Interest

The authors declare no competing financial interests

Funding Sources

This work was funded by the Army Research Office through the ARO-MURI program and ARO-Core grants (no. MURI W911NF-11-1-0024, ARO W911NF-09-1-0319).

ACKNOWLEDGEMENT

We appreciate the insightful conversations with D. Fishman, J. Hes, and D. Humphrey. SEM, TEM, and Oxygen Plasma work was performed at the Irvine Materials Research Institute (IMRI). Raman spectroscopy work was performed at the UC Irvine Laser Spectroscopy Facility (LSF). CVD Synthesis and E-Beam Evaporation was performed at the Integrated Nanosystems Research Facility (INRF).

REFERENCES

- (1) Li, X.; Cai, W.; An, J.; Kim, S.; Nah, J.; Yang, D.; Piner, R.; Velamakanni, A.; Jung, I.; Tutuc, E.; Banerjee, S. K.; Colombo, L.; Ruoff, R. S. Large-Area Synthesis of High-Quality and Uniform Graphene Films on Copper Foils. *Science* **2009**, *324*, 1312–1314.
- (2) Li, X.; Magnuson, C. W.; Venugopal, A.; Tromp, R. M.; Hannon, J. B.; Vogel, E. M.; Colombo, L.; Ruoff, R. S. Large-Area Graphene Single Crystals Grown by Low-Pressure Chemical Vapor Deposition of Methane on Copper. *J. Am. Chem. Soc.* **2011**, *133*, 2816–2819.
- (3) Li, X.; Magnuson, C. W.; Venugopal, A.; An, J.; Suk, J. W.; Han, B.; Borysiak, M.; Cai, W.; Velamakanni, A.; Zhu, Y.; Fu, L.; Vogel, E. M.; Voelkl, E.; Colombo, L.; Ruoff, R. S. Graphene Films with Large Domain Size by a Two-Step Chemical Vapor Deposition Process. *Nano Lett.* **2010**, *10*, 4328–4334.
- (4) Yu, Q.; Jauregui, L. A.; Wu, W.; Colby, R.; Tian, J.; Su, Z.; Cao, H.; Liu, Z.; Pandey, D.; Wei, D.; Chung, T. F.; Peng, P.; Guisinger, N. P.; Stach, E. A.; Bao, J.; Pei, S. S.; Chen, Y. P. Control and Characterization of Individual Grains and Grain Boundaries in Graphene Grown by Chemical Vapour Deposition. *Nat. Mater.* **2011**, *10*, 443–449.
- (5) Huang, P. Y.; Ruiz-Vargas, C. S.; van der Zande, A. M.; Whitney, W. S.; Levendorf, M. P.; Kevek, J. W.; Garg, S.; Alden, J. S.; Hustedt, C. J.; Zhu, Y.; Park, J.; McEuen, P. L.; Muller, D. A. Grains and Grain Boundaries in Single-Layer Graphene Atomic Patchwork Quilts. *Nature* **2011**, *469*, 389–392.
- (6) Chen, S.; Ji, H.; Chou, H.; Li, Q.; Li, H.; Suk, J. W.; Piner, R.; Liao, L.; Cai, W.; Ruoff, R. S. Millimeter-Size Single-Crystal Graphene by Suppressing Evaporative Loss of Cu

- 1
2
3 during Low Pressure Chemical Vapor Deposition. *Adv. Mater.* **2013**, *25*, 2062–2065.
- 4
5
6
7 (7) Yan, Z.; Lin, J.; Peng, Z.; Sun, Z.; Zhu, Y.; Li, L.; Xiang, C.; Samuel, E. L.; Kittrell, C.;
8
9 Tour, J. M. Toward the Synthesis of Wafer-Scale Single-Crystal Graphene on Copper
10
11 Foils. *ACS Nano* **2012**, *6*, 9110–9117.
- 12
13
14 (8) Hao, Y.; Bharathi, M. S.; Wang, L.; Liu, Y.; Chen, H.; Nie, S.; Wang, X.; Chou, H.; Tan,
15
16 C.; Fallahazad, B.; Ramanarayan, H.; Magnuson, C. W.; Tutuc, E.; Yakobson, B. I.;
17
18 McCarty, K. F.; Zhang, Y.; Kim, P.; Hone, J.; Colombo, L.; Ruoff, R. S. The Role of
19
20 Surface Oxygen in the Growth of Large Single-Crystal Graphene on Copper. *Science*
21
22 **2013**, *342*, 720–723.
- 23
24
25
26
27 (9) Zhou, H.; Yu, W. J.; Liu, L.; Cheng, R.; Chen, Y.; Huang, X.; Liu, Y.; Wang, Y.; Huang,
28
29 Y.; Duan, X. Chemical Vapour Deposition Growth of Large Single Crystals of Monolayer
30
31 and Bilayer Graphene. *Nat. Commun.* **2013**, *4*.
- 32
33
34
35 (10) Chen, X.; Zhao, P.; Xiang, R.; Kim, S.; Cha, J.; Chiashi, S.; Maruyama, S. Chemical
36
37 Vapor Deposition Growth of 5 Mm Hexagonal Single-Crystal Graphene from Ethanol.
38
39 *Carbon* **2015**, *94*, 810–815.
- 40
41
42
43 (11) Li, J.; Wang, X.-Y.; Liu, X.; Jin, Z.; Wang, D.; Wan, L. Facile Growth of Centimeter-
44
45 Sized Single-Crystal Graphene on Copper Foil at Atmospheric Pressure. *J. Mater. Chem.*
46
47 *C* **2015**, *3*, 3530–3535.
- 48
49
50
51 (12) Gan, L.; Luo, Z. Turning off Hydrogen to Realize Seeded Growth of Subcentimeter
52
53 Single-Crystal Graphene Grains on Copper. *ACS Nano* **2013**, *7*, 9480–9488.
- 54
55
56
57 (13) Kim, H.; Mattevi, C.; Calvo, M. R.; Oberg, J. C.; Artiglia, L.; Agnoli, S.; Hirjibehedin, C.
58
59
60

- 1
2
3 F.; Chhowalla, M.; Saiz, E. Activation Energy Paths for Graphene Nucleation and Growth
4 on Cu. *ACS Nano* **2012**, *6*, 3614–3623.
5
6
7
8
9 (14) Hao, Y.; Wang, L.; Liu, Y.; Chen, H.; Wang, X.; Tan, C.; Nie, S.; Suk, J. W.; Jiang, T.;
10 Liang, T.; Xiao, J.; Ye, W.; Dean, C. R.; Yakobson, B. I.; Mccarty, K. F.; Kim, P.; Hone,
11 J.; Colombo, L.; Ruoff, R. S. Oxygen-Activated Growth and Bandgap Tunability of Large
12 Single-Crystal Bilayer Graphene. *Nat. Nanotechnol.* **2016**, *11*, 426–231.
13
14
15
16
17
18
19 (15) Li, X.; Cai, W.; Colombo, L.; Ruoff, R. S. Evolution of Graphene Growth on Ni and Cu
20 by Carbon Isotope Labeling. *Nano Lett.* **2009**, *9*, 4268–4272.
21
22
23
24
25 (16) Wang, H.; Wang, G.; Bao, P.; Yang, S.; Zhu, W.; Xie, X.; Zhang, W. J. Controllable
26 Synthesis of Submillimeter Single-Crystal Monolayer Graphene Domains on Copper Foils
27 by Suppressing Nucleation. *J. Am. Chem. Soc.* **2012**, *134*, 3627–3630.
28
29
30
31
32
33 (17) Reina, A.; Son, H.; Jiao, L.; Fan, B.; Dresselhaus, M. S.; Liu, Z.; Kong, J. Transferring
34 and Identification of Single- and Few-Layer Graphene on Arbitrary Substrates
35 Transferring and Identification of Single- and Few-Layer Graphene on Arbitrary
36 Substrates. *J. Phys. Chem. C* **2008**, *112*, 17741–17744.
37
38
39
40
41
42
43 (18) Suk, J. W.; Kitt, A.; Magnuson, C. W.; Hao, Y.; Ahmed, S.; An, J.; Swan, A. K.;
44 Goldberg, B. B.; Ruoff, R. S. Transfer of CVD-Grown Monolayer Graphene onto
45 Arbitrary Substrates. *ACS Nano* **2011**, *5*, 6916–6924.
46
47
48
49
50
51 (19) Meyer, J. C.; Geim, A. K.; Katsnelson, M. I.; Novoselov, K. S.; Booth, T. J.; Roth, S. The
52 Structure of Suspended Graphene Sheets. *Nature* **2007**, *446*, 60–63.
53
54
55
56
57 (20) Lee, W. H.; Park, J.; Kim, Y.; Kim, K. S.; Hong, B. H.; Cho, K. Control of Graphene
58
59
60

- 1
2
3 Field-Effect Transistors by Interfacial Hydrophobic Self-Assembled Monolayers. *Adv.*
4
5
6 *Mater.* **2011**, *23*, 3460–3464.
7
8
9 (21) Ferrari, A. C.; Meyer, J. C.; Scardaci, V.; Casiraghi, C.; Lazzeri, M.; Mauri, F.; Piscanec,
10
11 S.; Jiang, D.; Novoselov, K. S.; Roth, S.; Geim, A. K. Raman Spectrum of Graphene and
12
13 Graphene Layers. *Phys. Rev. Lett.* **2006**, *97*, 1–4.
14
15
16 (22) Pirkle, A.; Chan, J.; Venugopal, A.; Hinojos, D.; Magnuson, C. W.; McDonnell, S.;
17
18 Colombo, L.; Vogel, E. M.; Ruoff, R. S.; Wallace, R. M. The Effect of Chemical Residues
19
20 on the Physical and Electrical Properties of Chemical Vapor Deposited Graphene
21
22 Transferred to SiO₂. *Appl. Phys. Lett.* **2011**, *99*, 2–5.
23
24
25 (23) Cancado, L. G.; Jorio, A.; Ferreira, E. H. M.; Stavale, F.; Achete, C. A.; Capaz, R. B.;
26
27 Moutinho, M. V. O.; Lombardo, A.; Kulmala, T. S.; Ferrari, A. C. Quantifying Defects in
28
29 Graphene via Raman Spectroscopy at Different Excitation Energies. *Nano Lett.* **2011**, *11*,
30
31 3190–3196.
32
33
34 (24) Das, A.; Pisana, S.; Chakraborty, B.; Piscanec, S.; Saha, S. K.; Waghmare, U. V.;
35
36 Novoselov, K. S.; Krishnamurthy, H. R.; Geim, A. K.; Ferrari, A. C.; Sood, A. K.
37
38 Monitoring Dopants by Raman Scattering in an Electrochemically Top-Gated Graphene
39
40 Transistor. *Nat. Nanotechnol.* **2008**, *3*, 210–215.
41
42
43 (25) Li, Q.; Chou, H.; Zhong, J. H.; Liu, J. Y.; Dolocan, A.; Zhang, J.; Zhou, Y.; Ruoff, R. S.;
44
45 Chen, S.; Cai, W. Growth of Adlayer Graphene on Cu Studied by Carbon Isotope
46
47 Labeling. *Nano Lett.* **2013**, *13*, 486–490.
48
49
50 (26) Zhang, W.; Wu, P.; Li, Z.; Yang, J. First-Principles Thermodynamics of Graphene Growth
51
52
53
54
55
56
57
58
59
60

- 1
2
3 on Cu Surfaces. *J. Phys. Chem. C* **2011**, *115*, 17782–17787.
- 4
5
6
7 (27) Bhaviripudi, S.; Jia, X.; Dresselhaus, M. S.; Kong, J. Role of Kinetic Factors in Chemical
8 Vapor Deposition Synthesis of Uniform Large Area Graphene Using Copper Catalyst.
9
10
11 *Nano Lett.* **2010**, *10*, 4128–4133.
- 12
13
14 (28) Loginova, E.; Bartelt, N. C.; Feibelman, P. J.; McCarty, K. F. Evidence for Graphene
15 Growth by C Cluster Attachment. *New J. Phys.* **2008**, *10*.
- 16
17
18
19 (29) Zhao, Z.; Shan, Z.; Zhang, C.; Li, Q.; Tian, B.; Huang, Z.; Lin, W.; Chen, X.; Ji, H.;
20 Zhang, W.; Cai, W. Study on the Diffusion Mechanism of Graphene Grown on Copper
21 Pockets. *Small* **2015**, *11*, 1418–1422.
- 22
23
24
25
26
27 (30) Losurdo, M.; Giangregorio, M. M.; Capezzuto, P.; Bruno, G. Graphene CVD Growth on
28 Copper and Nickel: Role of Hydrogen in Kinetics and Structure. *Phys. Chem. Chem. Phys.*
29
30
31
32 **2011**, *13*, 20836.
- 33
34
35 (31) Zhang, X.; Wang, L.; Xin, J. H.; Yakobson, B. I.; Ding, F. Role of Hydrogen in Graphene
36 Chemical Vapor Deposition Growth on a Copper Surface. *J. Am. Chem. Soc.* **2014**, *136*,
37
38
39
40
41
42 3040–3047.
- 43
44 (32) Riikonen, S.; Krasheninnikov, A. V.; Halonen, L.; Nieminen, R. M. The Role of Stable
45 and Mobile Carbon Adspecies in Copper-Promoted Graphene Growth. *J. Phys. Chem. C*
46
47
48
49 **2012**, *116*, 5802–5809.
- 50
51 (33) Gao, J.; Yip, J.; Zhao, J.; Yakobson, B. I.; Ding, F. Graphene Nucleation on Transition
52 Metal Surface: Structure Transformation and Role of the Metal Step Edge. *J. Am. Chem.*
53
54
55
56
57
58
59
60 *Soc.* **2011**, *133*, 5009–5015.

- 1
2
3
4
5
6
7
8
9
10
11
12
13
14
15
16
17
18
19
20
21
22
23
24
25
26
27
28
29
30
31
32
33
34
35
36
37
38
39
40
41
42
43
44
45
46
47
48
49
50
51
52
53
54
55
56
57
58
59
60
- (34) Artyukhov, V. I.; Liu, Y.; Yakobson, B. I. Equilibrium at the Edge and Atomistic Mechanisms of Graphene Growth. *Proc. Natl. Acad. Sci.* **2012**, *109*, 15136–15140.
- (35) Yuan, Q.; Yakobson, B. I.; Ding, F. Edge-Catalyst Wetting and Orientation Control of Graphene Growth by Chemical Vapor Deposition Growth. *J. Phys. Chem. Lett.* **2014**, *5*, 3093–3099.
- (36) Artyukhov, V. I.; Hao, Y.; Ruoff, R. S.; Yakobson, B. I. Breaking of Symmetry in Graphene Growth on Metal Substrates. *Phys. Rev. Lett.* **2015**, *114*, 1–6.
- (37) Gao, L.; Ren, W.; Xu, H.; Jin, L.; Wang, Z.; Ma, T.; Ma, L.-P.; Zhang, Z.; Fu, Q.; Peng, L.-M.; Bao, X.; Cheng, H.-M. Repeated Growth and Bubbling Transfer of Graphene with Millimetre-Size Single-Crystal Grains Using Platinum. *Nat. Commun.* **2012**, *3*, 699.
- (38) Loginova, E.; Bartelt, N. C.; Feibelmarr, P. J.; McCarty, K. F. Factors Influencing Graphene Growth on Metal Surfaces. *New J. Phys.* **2009**, *11*.
- (39) Kwon, S. Y.; Ciobanu, C. V.; Petrova, V.; Shenoy, V. B.; Bareño, J.; Gambin, V.; Petrov, I.; Kodambaka, S. Growth of Semiconducting Graphene on Palladium. *Nano Lett.* **2009**, *9*, 3985–3990.
- (40) Kim, K. S. K. S.; Zhao, Y.; Jang, H.; Lee, S. Y.; Kim, J. M.; Ahn, J.; Kim, P.; Choi, J.-Y.; Hong, B. H. Large-Scale Pattern Growth of Graphene Films for Stretchable Transparent Electrodes. *Nature* **2009**, *457*, 706–710.
- (41) Iwasaki, T.; Park, H. J.; Konuma, M.; Lee, D. S.; Smet, J. H.; Starke, U. Long-Range Ordered Single-Crystal Graphene on High-Quality Heteroepitaxial Ni Thin Films Grown on MgO(111). *Nano Lett.* **2011**, *11*, 79–84.

- 1
2
3 (42) Pan, Y.; Zhang, H.; Shi, D.; Sun, J.; Du, S.; Liu, F.; Gao, H. J. Highly Ordered,
4 Millimeter-Scale, Continuous, Single-Crystalline Graphene Monolayer Formed on Ru
5
6
7
8 (0001). *Adv. Mater.* **2009**, *21*, 2777–2780.
9
10
11
12
13
14
15
16
17
18
19
20
21
22
23
24
25
26
27
28
29
30
31
32
33
34
35
36
37
38
39
40
41
42
43
44
45
46
47
48
49
50
51
52
53
54
55
56
57
58
59
60

1
2
3 For Table of Contents Only
4
5
6

